Installation Effects of Ultrasonic Flowmeter in Single Bend Pipe

Dan-dan Zheng[1], Tao Zhang[1], Li-jun Sun[1]
Tao Meng[2], He-ming Hu[2], Chi Wang[2]
1. Tianjin Key Laboratory of Process Measurement and Control, School of Electrical Engineering & Automation, Tianjin University, Tianjin 300072, China
Phone:86-022-81287825, E-mail:zhengdandan@tju.edu.cn

2. National Institute of Metrology of China, Beijing 100013, China

Abstract: The downstream flow of 90°single bend was investigated by computational fluid dynamics (CFD). An acoustic transit time flowmeter was exposed to the downstream flow at various positions. Measurement errors with different meter configurations and effects of pipe wall roughness were discussed. Numerical simulation results of three diameter pipes 0.1m, 1m and 10m with increasing the roughness from 0 to 1mm were presented within Reynolds number (Re) range from 5×10^3 to 5×10^6.

Keywords: Ultrasonic flowmeter, Installation effect, Single bend pipe

1. Introduction

With advantages of no wear, non-intrusive and high accuracy, ultrasonic flowmeters have been developing fast in recent years. A.G.A Report No.9 is evidence of the interest that the gas industry has in ultrasonic flowmeters [1]. Besides, the use of multipath acoustic transit time flowmeters has gained acceptance for turbine performance testing and hydroelectric plant optimization in applications world wide [2]. It is known that ultrasonic flow measurement can provide an accuracy of up to ±0.5%. However, these accuracies can only be achieved if the installation of the flowmeter is carefully executed. Limited by spaces and cost, industrial applications of flow measurement do not have the luxury of long straight pipes thus often the flow entering the flowmeter is distorted, which influence the overall accuracy of ultrasonic flowmeter very strongly. It is of major interest for manufacturers and customers to know before the actual installation how the meter reacts to a specific flow disturbance.

Experiments for studying installation effects on ultrasonic flowmeter were proceeded consecutively in the past decade. A series of experiments were carried out by National Engineering Laboratory (NEL) in typical pipe configurations including contraction, expansion, single bend, twisted double bend and twisted triple bend [3-5]. Six ultrasonic floweters with various acoustic path number and configurations were tested in water and oil flow calibration loops respectively. Besides, experiments were done in large flows of high pressure natural gas to investigate the use of multipath flowmeters by Dell'Isola [6]. However, experimental investigations are time-consuming and very expensive. The knowledge of the flow field is in most cases restricted to several measurement traverses or measurement planes. A complete set of three-dimensional flow data in a pipe is very difficult to obtain.

A method for modeling and analyzing the effect of theoretical asymmetric flow profiles produced by Salami [7] on ultrasonic flowmeters were investigated to understand installation effects. The technique used to combine the profiles discussed with ultrasonic flowmeter path configurations of the transit-time type were described by P. I. Moore [8]. Also the theoretical model was used to study installation effects caused by wall roughness changes [9].Although theoretical method is much flexibility and less time-consuming, the analytical profiles must be supported by

experimental verification. Moreover, these profiles are two-dimensional description, which do not reflect the real disturbed flow completely.
With development of computer science, numerical simulation provides an efficient and comprehensive alternative on installation effect research. The results of computational fluid dynamics (CFD) simulations were compared against the test data to evaluate the applications and limits of CFD firstly. And then installation effects on ultrasonic flowmeters with various configurations were predicted by simulations [3, 4, 10]. Although for some installations, there was difference of a few percent between measured and calculated meter errors, trends were well represented, which was helpful for manufacturers and customers to use ultrasonic flowmeters.
In this work, the downstream flow of a typical installation in water piping system, the 90°single bend, will be investigated by CFD simulations using Fluent, which the information obtained is much more extensive than in experimental investigations. An acoustic transit time flowmeter is exposed to the downstream flow at various positions. At each position the measurement error with different ultrasonic flowmeter configurations are discussed respectively, such as the number of acoustic path, mounting angle and arrangement of acoustic measurement planes. Moreover, effects of pipe wall roughness are also analyzed. Particular and comprehensive results of installation effect are given at last, which can be as references for manufacturers and customers of ultrasonic flowmeter..

2. Ultrasonic flowmeter model

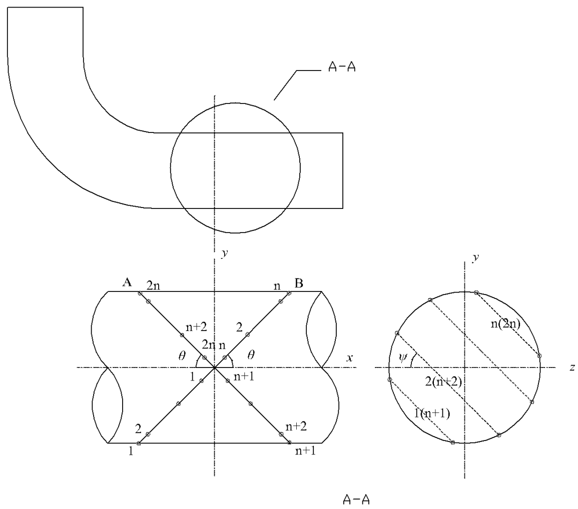

Fig.1 Arrangement of acoustic paths in single bend pipe

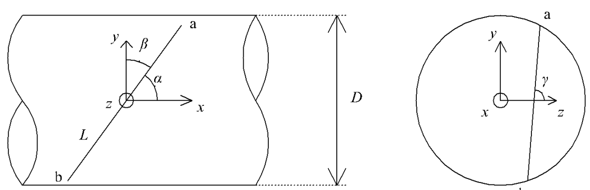

Fig.2 Velocity measurement along each path

As shown in Figure 1, the transit-time ultrasonic flowmeter is installed downtream of a single bend. The radius of curvature is *D*, which is the diameter of pipe. It has one or two (across) acoustic measurement planes (A, B) with *n* chordal paths each. The angle θ is 45°. ψ is mounting angle. Various measurement results are obtained with different ψ . To one acoustic path shown in Figure 2, the mean axial velocity components are given by

$$\overline{V}_{xi} = \frac{1}{L_i}\int_a^b v_{xi}dL \quad \overline{V}_{yi} = \frac{1}{L_i}\int_a^b v_{yi}dL \quad \overline{V}_{zi} = \frac{1}{L_i}\int_a^b v_{zi}dL \tag{1}$$

Where, L_i is length of path *i*. v_{xi} 、 v_{yi} 、 v_{zi} are instantaneous velocity components along path. Therefore, the average velocity along path *i* as calculated from measured transit times can be obtained.

$$V_i = \overline{V}_{xi} + \overline{V}_{yi}\frac{\cos\beta}{\cos\alpha} + \overline{V}_{zi}\frac{\cos\gamma}{\cos\alpha} = \overline{V}_{xi} + \overline{V}_{yi}\frac{y}{x} + \overline{V}_{zi}\frac{z}{x} \tag{2}$$

According to operating principle of multipath ultrasonic flowmeter [11], flowrate is calculated for one measurement acoustic plane.

$$Q = Q_{A/B} = \frac{D}{2}\sum_{i=1}^{n} W_i V_i L_i \sin\theta \tag{3}$$

Where, W_i is weighting coefficients depending on the number of path and integration technique used. In the paper, Jacobi-Gauss method [12] is adopted.

For two across planes, the flowrate is

$$Q = (Q_A + Q_B)/2 \tag{4}$$

In order to evaluate installation effect of ultrasonic flowmeter with different configurations, measurement error is defined.

$$e = \frac{Q - Q_t}{Q_t} \times 100\% \tag{5}$$

Where, Q_t is calculated from ultrasonic flowmeter with 36 chordal paths using the same method presented above. In this way, system error from CFD and post process method can be reduced. The true value of flowrate can be reflected by integration result of 36 paths which is already insensitive to disturbed flow.

3. Numerical simulation

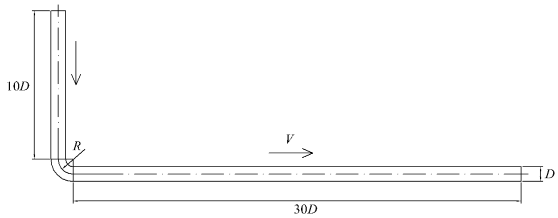

Fig.3 Computational domain of model

The computational domain is shown in Figure 3, where upstream length is 10*D* and downstream is 30*D*. *R*=*D*. Structured hexahedral meshes are created using Gambit. Boundary layers are added downstream of the bend, which can get more nodes near the wall where large velocity magnitude exists. The flow is modeled using Fluent. The inlet boundary condition is defined as uniform flow. To minimize numerical errors in the solution, the QUICK discretisation scheme is used. The fluid is water at standard pressure and temperature. Turbulence model plays an important role in simulation. Through comparing results using different turbulence models to experimental data given by NEL [6], the Reynolds stress model (RSM) is executed for all simulations. Comparison result is shown in Figure 4.

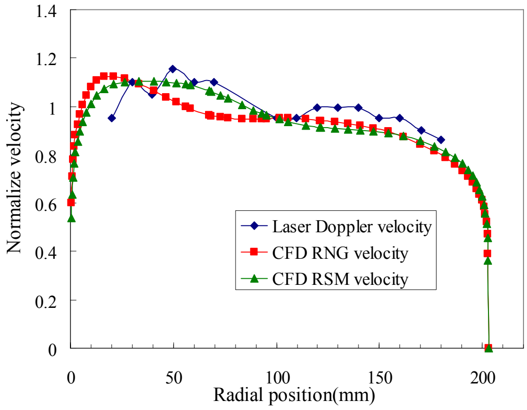

Fig.4 Comparison of turbulence models

4. Simulation results and analysis

Ultrasonic flowmeters with three diameters 0.1m, 1m and 10m are mainly discussed. Reynolds number (*Re*) range is from 5×10^3 to 5×10^6. Pipe wall roughness *Ra* is from 0 to 1mm. Five influencing factors—number of acoustic path, mounting angle, number of acoustic measurement plane, wall roughness and position downstream of the bend—are analyzed respectively.

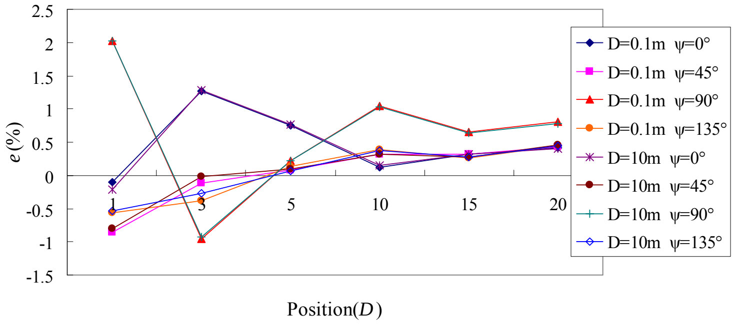

Fig.5 Re=5×10^6, 8 acoustic paths (two measurement planes with 4 chordal paths each)

Figure 5 shows measurement errors at different locations downstream of the bend with two pipes in the same *Re*. It is indicated that different flow conditions with same *Re* have equal measurement error when having the same meter configuration, which meets the Reynolds criterion of viscous similarity. In other *Re* range, the same conclusion is obtained. Besides, it is found that the results are almost same with mounting angle $\psi = 45^\circ$ and $\psi = 135^\circ$. It is explained that a double symmetric vortex pattern is generated downstream of the bend shown in Figure 6.

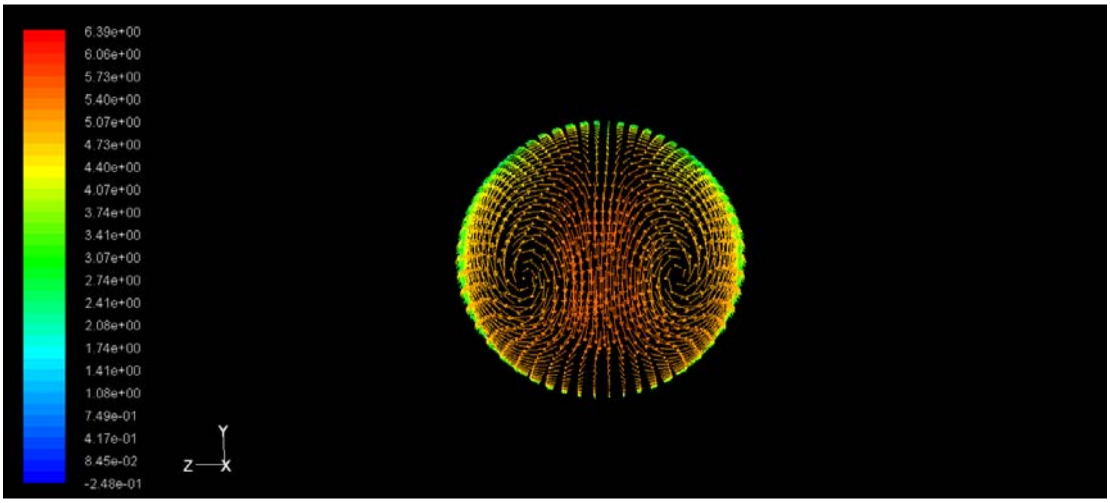

Fig.6 Axial velocity vectors downstream of the bend

Based on Reynolds similarity, simulation results on diameter 0.1m pipe flow conditions are mainly discussed. The velocity range is from 0.05m/s to 50m/s and *Re* is from 5×10^3 to 5×10^6.

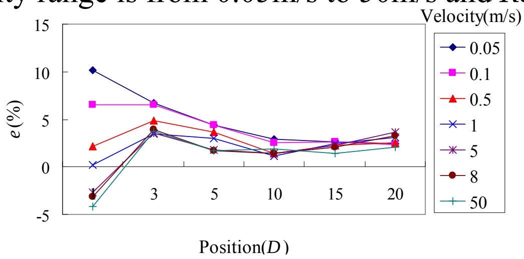

Fig.7 One plane with 2 paths

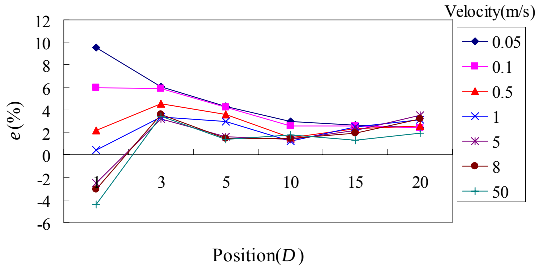

Fig.8 Two planes with 2 paths each

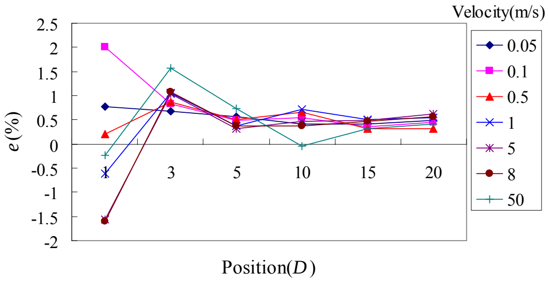

Fig.9 One plane with 4 paths

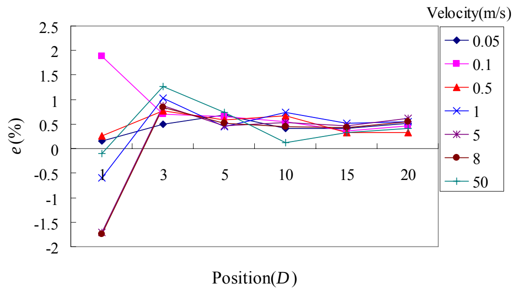

Fig.10 Two planes with 4 paths each

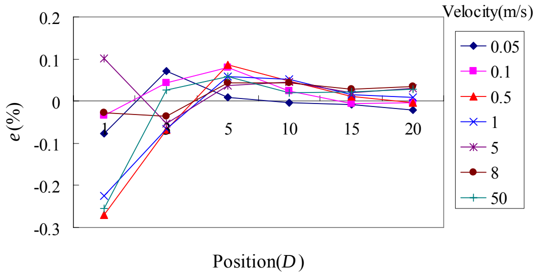

Fig.11 One plane with 9 paths

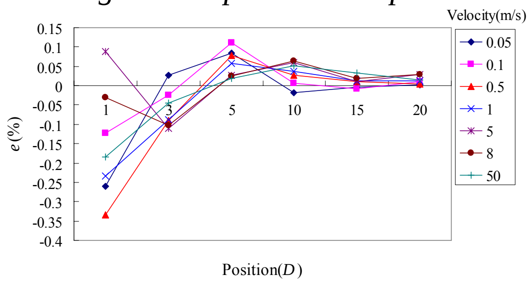

Fig.12 Two planes with 9 paths each

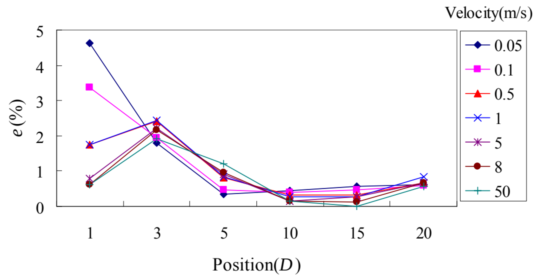

Fig.13 One plane with 4 paths, $\psi = 45^\circ$

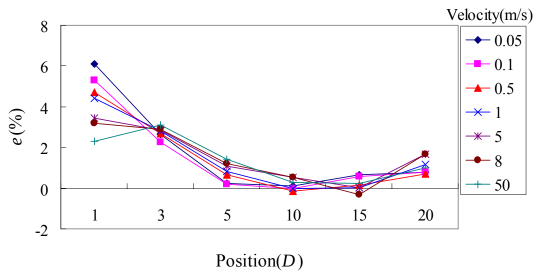

Fig.14 One plane with 4 paths, $\psi = 90^\circ$

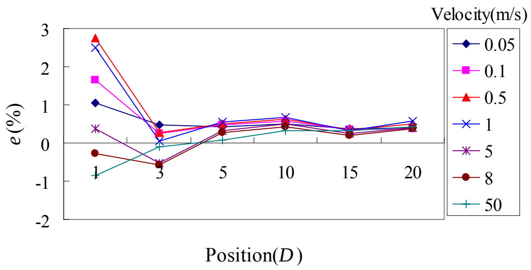

Fig.15 Two plane with 4 paths each, $\psi = 45^\circ$

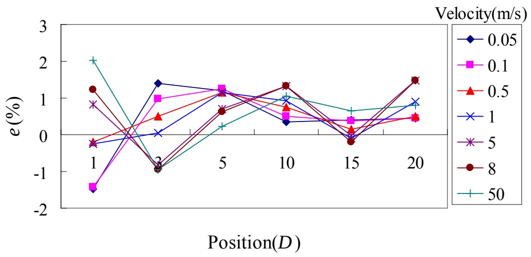

Fig.16 Two plane with 4 paths each, $\psi = 90^\circ$

Figure 7-12 shows measurement errors using one/two measurement planes with different acoustic path number respectively and $\psi = 0^\circ$. To one measurement plane, 2 paths arrangement is not enough for accurate measurement shown in Figure 7. With path number increasing, measurement errors are decreased. As shown in Figure 9, the accuracy is about ±0.5% after 5*D* when 4 paths are used. And ±0.2% is obtained after 3*D* when 9 paths are configured in one plane shown in Figure 11. Measurement errors are reduced gradually with positions going away bend, where vortices decays, not matter how many paths are used. Moreover, mounting angle effects with one measurement plane are shown in Figure 13 and 14. Various mounting angles affect the measurement errors apparently within 5*D* length downstream of the bend where secondary flow is strong. Through comparing 0°, 45°and 90°, relative small error can be obtained when mounting angle is 0°. 90°is the worst conversely. In contrast to one plane configuration, two across planes have nearly the same accuracy with one acoustic plane. However, two plane configurations are not very sensitive to mounting angle shown in Figure 10, 15 and 16, which indicates that measurement error caused by secondary flow downstream of single bend is strongly reduced by two across planes. It is worth noticing that there is no regularity of measurement error change with *Re* increasing especially near the bend, which reflects that the flow field is complex. Results shown above are focused on smooth pipe condition where *Ra*=0. To real flow in pipe, wall roughness must be considered. The influences are discussed below.

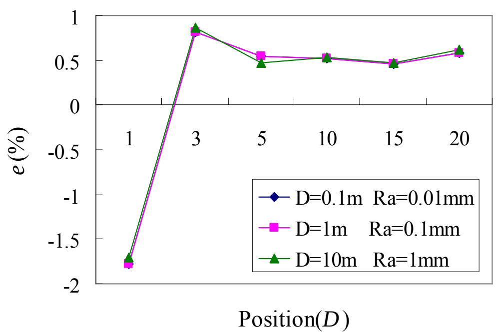

Fig.17 Two planes with 4 paths each, Re=5×10^5, $\psi = 0^\circ$

Figure 17 shows measurement errors with same *Re* and relative wall roughness *r* defined by $\frac{Ra}{D}$. Three error curves are almost the same. Based on this conclusion, flow conditions simulated can be largely reduced. Figure 18-20 shows results with different mounting angle when *D*=1m, *Re*=5×10^5 and *r* is from 0 to 5×10^{-4}. The influences of pipe wall roughness appear various. The effects are not obvious with $\psi = 0^\circ$ and errors are equal to one of smooth pipe. Conversely, at $\psi = 45^\circ$ and $\psi = 90^\circ$, measurement accuracy is changed much with wall roughness increasing especially within 3*D* length downstream of the bend. Moreover, trends of error shift are different with various mounting angles. In order to quantify the influence of wall roughness, a critical relative roughness is given, which means that pipe wall roughness can not be neglected when *r* is larger than this value. References to Figure 18, 19 and 20, the critical value is about $\frac{0.2mm}{1000mm} = 2\times10^{-4}$. It is worth emphasizing that the value is more important within 3*D* range where secondary flow is strong. With going downstream the bend, roughness effects gradually decays.

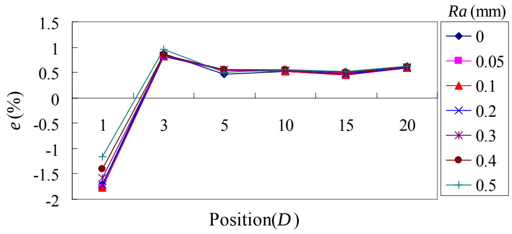

Fig.18 Two planes with 4 paths each, D=1m, Re=5×10^5, $\psi = 0^\circ$

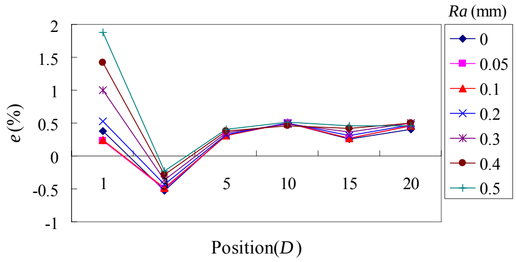

Fig.19 Two planes with 4 paths each, D=1m, Re=5×10^5, $\psi = 45^\circ$

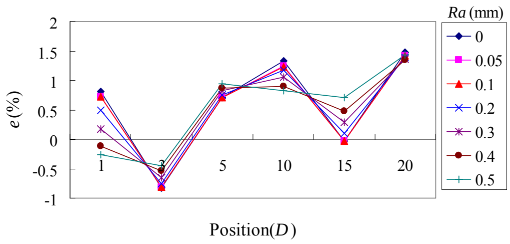

Fig.20 Two planes with 4 paths each, D=1m, Re=5×10^5, $\psi = 90^\circ$

5. Conclusions

Through numerical simulations on different flow conditions with various ultrasonic flowmeter configurations, five conclusions are summarized below.

1. With one acoustic plane, the accuracy of ultrasonic flowmeter can be achieved ±0.5% when the flowmeter should have at least 4 acoustic paths and installed at least 5*D* downstream of the bend. The ±0.2% can be reached at least 3*D* downstream with 9 acoustic paths in one

plane. The most important for one acoustic measurement plane is the mounting angle. 0°is the best while 90°is the worst.

2. In contrast to one acoustic plane, ultrasonic flowmeter with two across measurement planes has the same accuracy with one acoustic plane. However, it is not very sensitive to mounting angle, which indicates that the measurement error caused by secondary flow downstream of single bend is strongly reduced by two across planes.
3. Different flow conditions with same *Re* have equal measurement error. With this conclusion, the number of numerical simulations can be decreased and time is saved.
4. The measurement accuracy is influenced by pipe wall roughness only in 3*D* length downstream of the bend, while this effect can be neglected after 3*D* in most cases. Within 3*D* near the bend, a critical relative roughness 2×10^{-4} is given. It means that wall roughness should be paid attention when ratio between wall roughness and pipe diameter is larger than this value.
5. Different flow conditions with same *Re* and relative wall roughness have equal measurement accuracy.

References

[1] Measurement of gas by multipath ultrasonic meters [R], American Gas Association. A. G. A. Report No.9, 1998
[2] J. T. Walsh, A report of acoustic transit time accuracy field work performed in North America [C], 5th International Conference on Hydraulic Efficiency Measurements, Lucerne, 2004
[3] N. A. Barton, G. J. Brown, Velocity distribution effects on ultrasonic flowmeters—Part 2 Determination by computational and experimental methods [R], Report No. 348/99, National Engineering Laboratory, 1999
[4] N. A. Barton, D. Boam, In-service performance of ultrasonic flowmeters—Application and validation of CFD modeling methods [R], Report No. 2002/72, National Engineering Laboratory, 2002
[5] C. J. Coull, D. Boam, In-Service performance of ultrasonic flowmeters—Investigation of installation effect [R], Report No. 2002/55, National Engineering Laboratory, 2002
[6] Marco Dell'Isola, Mauro Cannizzo, Matteo Diritti, Measurement of high-pressure natural gas flow using ultrasonic flowmeters, Measurement, 20(2) 1997: 75-89
[7] Salami L. A., Application of a computer to asymmetric flow measurement in circular pipes, Trans. Inst. Meas. Control, 1984, 6: 197-206
[8] P. I. Moore, G. J. Brown, B. P. Stimpson, Ultrasonic transit-time flowmeters modeled with theoretical velocity profiles: methodology, Meas. Sci. Technol. 11(2000): 1802-1811
[9] A. Calogirou, J. Boekhoven, R. A. W. M. Henkes, Effects of wall roughness changes on ultrasonic gas flowmeters, Flow Meas. Instrum., 12(2001): 219-229
[10] Martin Holm, Jacob Stang, Jerker Delsing, Simulation of flow meter calibration factors for various installation effects, Measurment, 15(1995): 235-244
[11] ASME PTC 18-2002, Hydraulic turbines and pump-turbines [S]
[12] W.H. Press, S. A. Teukolsky, Numerical Recipes in C [M], Cambridge University Press, 1992: 147-156.